

Thermodynamic Analyses of the Structure and Growth of Asymmetric Linear Short-Chain Lecithin Micelles Based on Small-Angle Neutron Scattering Data

Tsang-Lang Lin,^{†,§} Sow-Hsin Chen,^{*†} and Mary F. Roberts^{‡,⊥}

Contribution from the Department of Nuclear Engineering and Department of Chemistry, Massachusetts Institute of Technology, Cambridge, Massachusetts 02139.

Received September 17, 1986

Abstract: Small-angle neutron scattering data for a series of five asymmetric short-chain lecithins in aqueous solutions are analyzed in terms of a thermodynamic model for a system of spherocylindrical micelles. This analysis yields five parameters which uniquely characterize the micellar system formed by each lecithin: N_0 , the aggregation number of the minimum size micelle; δ/kT , the free energy change for a monomer when it is inserted into the cylindrical section of the micelle; Δ/kT , the free energy change when N_0 monomers aggregate to form a minimum size micelle; R_c , the transverse radius of gyration; and N/L , the aggregation number per unit micelle length. Growth from the minimum micelle size is determined by the difference in free energy of monomers in the end caps vs. the same number of monomers in the cylindrical section, $(\Delta - N_0 \delta)/kT$. This value is related to the total number of carbons in the fatty acyl chains. It is estimated to be 7 for dihexanoylphosphatidylcholine (12 carbons) and increases to 12, 16, and 23 for lecithins with 13, 14, and 15 carbons, respectively. The conformational nonequivalence of the two fatty acyl chains affects the critical micelle concentrations, the average micelle sizes, and hence the extracted free energy parameters. For compounds with the same total number of fatty acyl carbons, the longer S_{N1} chain species produce smaller, more slowly growing micelles with slightly lower critical micelle concentrations. This can be understood if the short-chain lecithin molecule in micelles assumes a conformation similar to that of the long-chain lecithin in bilayers. ¹H NMR data assessing the magnetic nonequivalence of the terminal methyl groups are consistent with this view.

Synthetic short-chain lecithins (1,2-diacyl-*sn*-glycero-3-phosphocholines with six to eight carbons in each fatty acyl linkage) are useful model phospholipids. In aqueous solution they form micelles (rather than the multibilayers formed by longer chain phospholipids) whose properties (critical micelle concentration, average size, shape) depend on the total number of carbons in the fatty acyl linkages.¹⁻³ Symmetric short-chain lecithins (where both S_{N1} and S_{N2} fatty acids are identical) have been studied in detail by a number of spectroscopic techniques.⁴⁻⁷ Dihexanoylphosphatidylcholine (dihexanoyl-PC, where PC = phosphatidylcholine) micelles grow at most from 18 to 20 monomers as the lecithin concentration is increased from 27 to 360 mM.⁷ When one methylene is added to each chain the resultant lecithin, diheptanoyl-PC, forms micelles which grow rapidly (as monitored by quasi-elastic light scattering⁶ and small-angle neutron scattering studies⁸) with increasing lecithin concentration. The next lecithin in this series, dioctanoyl-PC, forms tremendously large micelles.^{3,6}

We have derived a model for short-chain lecithin micelles which treats them as spherocylinders that grow in the longitudinal direction with increasing lecithin concentration. The growth is due to the free energy of insertion of a monomer in the straight section of the spherocylindrical micelle being lower than that in the end caps of the micelle.⁸ This free energy difference is attributed to the smaller surface area of the hydrocarbon core in contact with water for a monomer in the straight section compared to that in the end caps. Micellar growth measured in terms of the increase in the weight-averaged aggregation number \bar{N} is roughly proportional to the square root of the micellar concentration $(X - X_1)^{1/2}$, where X is the total lecithin concentration in mole fraction and X_1 is the concentration (in mole fraction) of lecithins in the free monomer state. The proportionality constant in the high concentration limit is equal to $2(e^{(\Delta - N_0 \delta)/kT})^{1/2}$, where $(\Delta - N_0 \delta)/kT$ is the total difference in free energy (TDF) in units of kT between the monomers in the two end caps and the same number of monomers in the straight section.⁸ It is assumed that micelles grow

from a minimum size of N_0 monomers by inserting more monomers into the center portion to form spherocylindrical micelles. Thus, N_0 is also the number of monomers forming the two end caps of a spherocylindrical micelle. δ/kT is the lowering of free energy in units of kT of a monomer when it is inserted into the cylindrical section of the spherocylindrical micelle, and Δ/kT is the corresponding free energy change in units of kT when N_0 free monomers form a minimum size micelle. For dihexanoyl-PC, which does not grow much, the TDF is estimated to be 7 with $N_0 = 19 \pm 1$; for diheptanoyl-PC, whose micelles grow significantly, TDF = 16.46 ± 0.02 and $N_0 = 27 \pm 1$.⁸

Further tests of this thermodynamic model can be made by SANS studies of other short-chain lecithins. Asymmetric lecithins have different length S_{N1} and S_{N2} acyl chains and more variability in the total number of fatty acyl carbons. It has been established that the two fatty acids of lecithins are nonequivalent in micelles^{4,5,9,10} as well as in bilayers.¹¹⁻¹³ This conformational difference may affect the thermodynamic parameters of the micelles. For example, 1-hexanoyl-2-octanoyl-PC and 1-octanoyl-2-hexanoyl-PC have the same total number of fatty acyl carbons (14) as diheptanoyl-PC but have acyl chains one carbon shorter and one carbon longer than the symmetric species. In forming micelles,

(1) Tausk, R. J. M.; Karmiggelt, J.; Oudshoorn, C.; Overbeek, J. Th. G. *Biophys. Chem.* **1974**, *1*, 175.

(2) Tausk, R. J. M.; Esch, J. van.; Karmiggelt, J.; Voordouw, G. Overbeek, J. Th. G. *Biophys. Chem.* **1974**, *1*, 184.

(3) Tausk, R. J. M.; Oudshoorn, C.; Overbeek, J. Th. G. *Biophys. Chem.* **1974**, *2*, 53.

(4) Burns, R. A., Jr.; Roberts, M. F. *Biochemistry* **1980**, *19*, 3100.

(5) Burns, R. A., Jr.; Roberts, M. F.; Dluhy, R.; Mendelsohn, R. *J. Am. Chem. Soc.* **1982**, *104*, 430.

(6) Burns, R. A., Jr.; Donovan, J. M.; Roberts, M. F. *Biochemistry* **1983**, *22*, 964.

(7) Lin, T.-L.; Chen, S.-H.; Gabriel, N. E.; Roberts, M. F. *J. Am. Chem. Soc.* **1986**, *108*, 3499.

(8) Lin, T.-L.; Chen, S.-H.; Gabriel, N. E.; Roberts, M. F. *J. Phys. Chem.* **1987**, *91*, 406.

(9) Roberts, M. F.; Bothner-By, A. A.; Dennis, E. A. *Biochemistry* **1978**, *17*, 935.

(10) DeBoese, C. D.; Burns, R. A., Jr.; Donovan, J. M.; Roberts, M. F. *Biochemistry* **1985**, *24*, 1298.

(11) Pearson, R. H.; Pascher, J. *Nature (London)* **1979**, *281*, 499.

(12) Buldt, G.; Gally, H. U.; Seelig, A.; Seelig, J. *Nature (London)* **1978**, *271*, 182.

(13) Seelig, J.; Browning, J. L. *FEBS Lett.* **1978**, *92*, 41.

[†] Department of Nuclear Engineering.

[‡] Department of Chemistry.

[§] Present address: Department of Nuclear Engineering, National Tsing-Hua University, Hsin-Chu, Taiwan, R.O.C.

[⊥] Present address: F. Bitter National Magnet Laboratory, M.I.T., Cambridge, MA 02139.

the minor radius of the hydrocarbon core of a globular micelle is expected to be as large as permissible and to stay in a circular or close to a circular form in order to minimize the ratio of the surface area of the hydrocarbon core in contact with water to its volume. For micelles formed by single fatty acyl chain surfactants, the minor radius of the hydrocarbon core is found to be equal to the fully stretched tail length,¹⁴ and the cross sectional area of the core is expected to have a circular form due to symmetric requirements. For surfactants with two fatty acyl chains the situation may be different from a single-chain case since the two chains of a surfactant are not completely independent of each other. Conformational differences in the lecithin S_{N1} and S_{N2} positions for a pair such as 1-hexanoyl-2-octanoyl-PC and 1-octanoyl-2-hexanoyl-PC should be reflected in micelle properties such as size, critical micelle concentration (CMC), etc.

The present article reports SANS studies of asymmetric short-chain lecithins including 1-hexanoyl-2-heptanoyl-PC, 1-hexanoyl-2-octanoyl-PC, 1-octanoyl-2-hexanoyl-PC, 1-heptanoyl-2-octanoyl-PC, and 1-octanoyl-2-heptanoyl-PC and their analyses in terms of the thermodynamic model. Together with ¹H NMR studies of these asymmetric species they confirm the nonequivalence of the S_{N1} and S_{N2} chains in lecithin micelles and provide a quantitative understanding of growth characteristics of these short-chain lecithins. The structural parameters derived for this series of compounds are useful in evaluating explanations for the higher enzymatic activity of water-soluble phospholipases toward lecithin in micelles as compared to lecithin in bilayers.^{15,16}

Experimental Section

Materials. Asymmetric linear lecithins 1-hexanoyl-2-heptanoyl-PC, 1-hexanoyl-2-octanoyl-PC, 1-octanoyl-2-hexanoyl-PC, 1-heptanoyl-2-octanoyl-PC, and 1-octanoyl-2-heptanoyl-PC were synthesized by reacting the appropriate lysophosphatidylcholine (obtained from Avanti Biochemicals, Birmingham, AL, or prepared by cobra venom phospholipase A_2 hydrolysis of the diacyl species) with the desired fatty acid activated by prior reaction with carbonyldiimidazole in $CHCl_3$.⁴ The acylation reaction was followed by thin-layer chromatography as described previously.⁴ Upon completion, the reaction mixtures were chromatographed on silicic acid by using methanol in acetone or methanol in chloroform gradients to purify the asymmetric lecithin from an unreacted lyso-PC and free fatty acid. The lyso lecithin was >95% of the 1-acyl-PC isomer. Samples of different concentrations from about 1.5 times the CMC to at least 5 times the CMC were prepared for each lecithin species. This ensures a suitable range of concentrations for testing the thermodynamic theory of micelle growth. Lecithin concentrations were all kept below 35 mM to ensure that the interaction between micelles can be neglected. Sample concentrations, both before and after SANS measurements, were determined by a colorimetric phosphate assay described previously.¹⁷ Uncertainty in lecithin concentration determined in this way was $\pm 2\%$.

Small-Angle Neutron Scattering. Most of the SANS spectra were obtained at the high flux beam reactor (HFBR) of Brookhaven National Laboratory. Samples were kept at 25 °C during the measurement. The sample to the 50×50 cm² position-sensitive detector distance was set at 1.76 m. The neutron beam employed in the scattering measurement had a wavelength $\lambda = 5.45$ Å with a spread $\Delta\lambda/\lambda \approx 10\%$. This arrangement allowed acquisition of small- Q data in the Q range 0.013–0.22 Å⁻¹. Q is the magnitude of the scattering vector given by $Q = 4\pi/\lambda \sin(\theta/2)$, where θ is the scattering angle. The measured neutron scattering intensity distributions were corrected for background, detector efficiency, contribution from the sample cell, and incoherent scattering of the sample and were normalized with scattering from a 1-mm water sample to obtain a scattering cross section per unit sample volume $J(Q)$ in a unit of 1/cm.¹⁸ For very small Q range, $0.005 \leq Q \leq 0.04$ (Å⁻¹), SANS spectra were acquired with a 30-M SANS instrument at the National Center for Small Angle Scattering Research located at the high flux isotope reactor of Oak Ridge National Laboratory.

NMR Spectroscopy. ¹H NMR spectra of asymmetric short-chain lecithins at 500 MHz were obtained on a home-built instrument at the F. Bitter National Magnet Laboratory of M.I.T. Typical parameters include 4000-Hz sweep width, 60° pulse width, 5-s recycle time, and exponential multiplication of the free induction decay by 2 Hz. Lecithin samples in D₂O were the ones used for SANS experiments as well as further diluted monomer samples of 0.05–0.2 mM. The chemical shifts (referenced to external Me₄Si) of the *N*-methyl, CH₂N, and POCH₂ groups were monitored as a function of lecithin concentration and were used to determine the CMC value for each lecithin.

SANS Analysis. The theory of micellar growth and the methods for analyzing SANS data for a polydisperse system have been presented in detail elsewhere.⁸ According to a phenomenological theory which is based on the "step and ladder" models of Benedek and co-workers,¹⁹ the formation and growth of micelles are characterized by three parameters, $(\Delta - N_0\delta)/kT$, δ/kT , and N_0 . These parameters together with the total lecithin concentration in the solution enable one to calculate the concentration (in mole fraction) distribution of the aggregates with *N*-mer, X_N , in equilibrium with monomer as given by⁸

$$X_N = N\beta^N e^{-(\Delta - N_0\delta)/kT} \quad N \geq N_0 \quad (1)$$

where

$$\beta \equiv X_1 e^{-\delta/kT} \quad (2)$$

The parameter β can be determined by using a constraint that the total concentration X in mole fraction is equal to the sum of all X_N 's and X_1 . This material balance equation⁸ is given in eq 3. The weight-averaged aggregation number \bar{N} at a given concentration is predicted to be eq 4.⁸

$$X = X_1 + e^{-(\Delta - N_0\delta)/kT} \left[N_0 \beta^{N_0} \left(\frac{1}{1 - \beta} + \frac{\beta}{N_0(1 - \beta)^2} \right) \right] \quad (3)$$

$$\bar{N} = N_0 + \frac{\beta}{1 - \beta} \left[1 + \frac{1}{N_0(1 - \beta) + \beta} \right] \quad (4)$$

The dependence of the weight-averaged aggregation number on the micellar concentration in this theory is given by eq 5.⁸ The β -dependent

$$\frac{\bar{N} - N_0}{(X - X_1)^{1/2}} = \frac{e^{(\Delta - N_0\delta)/2kT} \beta^{1 - N_0/2} \left[1 + \frac{1}{\beta + N_0(1 - \beta)} \right]}{[\beta + N_0(1 - \beta)]^{1/2}} \quad (5)$$

part of the right-hand side of eq 5 approaches 2 in the high concentration limit $\beta = 1$. But in general it is more accurate to use the complete equation even for the case when β is close to unity. It appears from this equation that $\bar{N} - N_0$ is roughly proportional to the square root of $(X - X_1)^{1/2}$.

The neutron scattering intensity at $Q = 0$, I_0 , for a dilute system, is directly proportional to the weight-averaged aggregation number \bar{N} , while the neutron scattering intensity profile depends on the polydispersity (size distribution) and the geometrical shape of the micelles in the solution. In general, the neutron scattering intensity distribution $I(Q)$ can be written as the product of I_0 and a normalized form factor $\bar{P}(Q)$ when the interaction between micelles can be neglected:

$$I(Q) = I_0 \bar{P}(Q) \quad (6)$$

where

$$I_0 = (C - C_1) \bar{N} (b_m - \rho_s V_m)^2 \quad (7)$$

C and C_1 are the total lecithin concentration and the free monomer concentration in units of molecules per unit volume, respectively. b_m is the coherent neutron scattering length of the lecithin molecule, and V_m is the dry volume of a lecithin molecule which can be computed for each lecithin species.⁸ ρ_s is the coherent neutron scattering length density of the solvent. It was shown that the diheptanoyl-PC forms spherocylindrical micelles, and a micelle can be modeled as a homogeneous cylinder in computing the normalized form factor $\bar{P}(Q)$.⁸ The cylinder can be specified by values of the length L and the radius R . Since the micelles grow only in the longitudinal direction, the cross sectional structure is similar and the parameter aggregation number per unit micelle length, N/L , is a constant for each lecithin micelle. Knowing the micelle concentration distribution, X_N , and the value of N/L , one is able to calculate the size (length) distribution of the micelles, which is then used to calculate the normalized structure factor. The spherocylindrical micelles have a transverse radius of gyration R_c which is related to the radius R of the cylinder by $R_c = R/2^{1/2}$.

Experimental data obtained for samples of five or more concentrations of a given lecithin species were fitted with this model to determine the

(14) Bendedouch, D.; Chen, S.-H.; Koehler, W. C. *J. Phys. Chem.* **1983**, *87*, 153.

(15) Kensil, C. A.; Dennis, E. A. *J. Biol. Chem.* **1979**, *254*, 5843.

(16) El-Sayed, M. Y.; DeBose, C. D.; Coury, L. A.; Roberts, M. F. *Biochim. Biophys. Acta* **1985**, *837*, 325.

(17) Eaton, B. R.; Dennis, E. A. *Arch. Biochem. Biophys.* **1976**, *176*, 604.

(18) Chen, S. H.; Lin, T.-L. In *Methods of Experimental Physics—Neutron Scattering*; Skold, K., Price, D. L., Eds.; Academic: New York, 1987; Vol. II.

(19) Missel, P. J.; Mazer, N. A.; Benedek, G. B.; Young, C. Y.; Carey, M. C. *J. Phys. Chem.* **1980**, *84*, 1044.

Table I. Parameters Derived from SANS Data Which Characterize Short-Chain Lecithin Micelles

lecithin	N_0	δ/kT	$(\Delta - N_0\delta)/kT$	$R_c, \text{\AA}$	$N/L, 1/\text{\AA}$
$(C_6)_2\text{-PC}^a$	16		7		
1- C_6 -2- C_7 -PC ^b	25 ± 2	-10.65 ± 0.02	12.09 ± 0.02	11.9	0.75 ± 0.07
$(C_7)_2\text{-PC}^c$	27 ± 1	-10.48 ± 0.02	16.46 ± 0.02	12.7	0.75 ± 0.02
1- C_6 -2- C_8 -PC	32 ± 5	-10.57 ± 0.02	16.08 ± 0.03	12.6	0.85 ± 0.06
1- C_8 -2- C_6 -PC	27 ± 5	-10.68 ± 0.03	15.17 ± 0.02	12.7	0.82 ± 0.04
1- C_7 -2- C_8 -PC	48 ± 10	-11.20 ± 0.01	23.52 ± 0.05	15.2	1.06 ± 0.10
1- C_8 -2- C_7 -PC	45 ± 10	-11.34 ± 0.01	22.71 ± 0.05	13.8	0.94 ± 0.06

^a $(C_6)_2\text{-PC}$, dihexanoylphosphatidylcholine; parameters derived from SANS data presented in: Lin et al. *J. Am. Chem. Soc.* **1986**, *108*, 3499. ^b For 1- C_x -2- C_y -PC, x denotes the number of carbons in the fatty acid esterified to the S_{N1} position and y denotes the number of carbons in the fatty acid esterified to the S_{N2} position. ^c $(C_7)_2\text{-PC}$, diheptanoylphosphatidylcholine; parameters derived from SANS in: Lin et al. *J. Phys. Chem.* **1987**, *91*, 406.

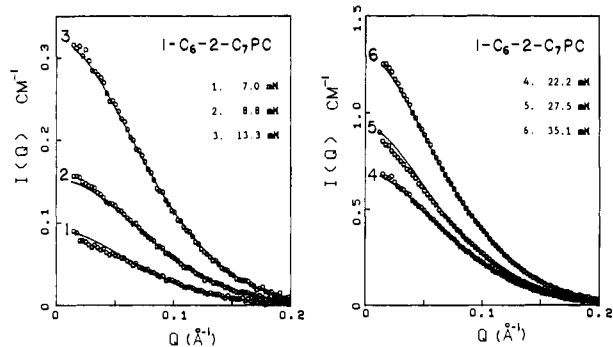


Figure 1. SANS data from 1-hexanoyl-2-heptanoyl-PC (1- C_6 -2- C_7 -PC) micellar solutions in D_2O . The solid lines are the fitted curves from the parameters listed in Table I.

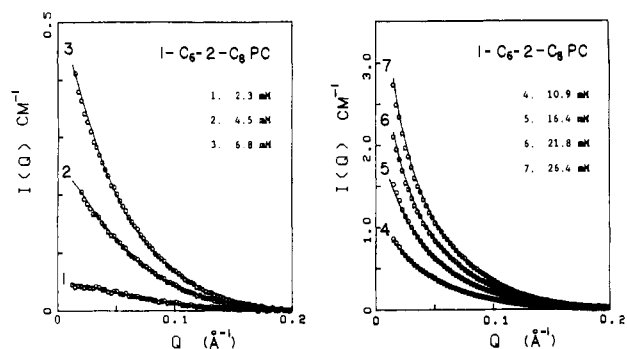


Figure 2. SANS data from 1-hexanoyl-2-octanoyl-PC (1- C_6 -2- C_8 -PC) micellar solutions in D_2O . The solid lines are the fitted curves from the parameters listed in Table I.

five parameters $(\Delta - N_0\delta)/kT$, δ/kT , N_0 , N/L , and R_c . The nonlinear least-squares fitting was done by first entering guessed initial values of these five parameters. The fitting routine then refines these parameters, and a converged set is obtained after some iterations. A comprehensive description of this process has been given by Lin et al.⁸

Results

Extrapolation of Micelle Parameters. Figure 1 shows SANS data from 1-hexanoyl-2-heptanoyl-PC micelles at different concentrations together with the fitted curves. The fitting results of other series, 1-hexanoyl-2-octanoyl-PC, 1-octanoyl-2-hexanoyl-PC, 1-heptanoyl-2-octanoyl-PC, and 1-octanoyl-2-heptanoyl-PC, are shown in Figures 2, 3, 4, and 5, respectively. In each series all the data from low to high concentrations are fitted very well by the cylinder model. The scattering intensity and profile of 1-hexanoyl-2-heptanoyl-PC micelles indicate that they do not grow much in this concentration range, 7–35.1 mM. In contrast, 1-hexanoyl-2-octanoyl-PC and 1-octanoyl-2-hexanoyl-PC micelles grow appreciably as indicated by the rapid increase of the scattering intensity in the small- Q region (Figures 2 and 3). For 1-heptanoyl-2-octanoyl-PC and 1-octanoyl-2-heptanoyl-PC micelles, the growth is even more pronounced. The scattering intensity is higher for 1-hexanoyl-2-octanoyl-PC compared with that for 1-octanoyl-2-hexanoyl-PC at the same concentration, and this is also true for 1-heptanoyl-2-octanoyl-PC compared with 1-oc-

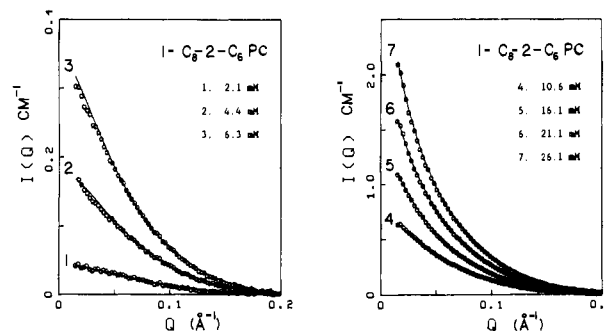


Figure 3. SANS data from 1-octanoyl-2-hexanoyl-PC (1- C_8 -2- C_6 -PC) micellar solutions in D_2O . The solid lines are the fitted curves from the parameters listed in Table I.

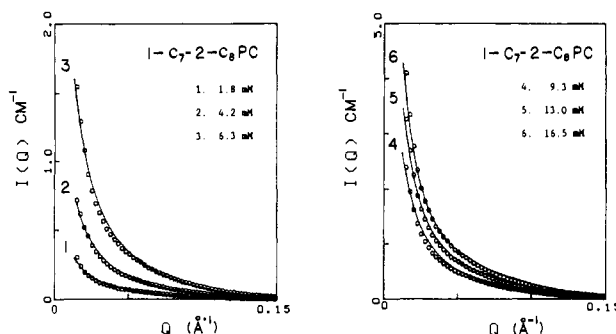


Figure 4. SANS data from 1-heptanoyl-2-octanoyl-PC (1- C_7 -2- C_8 -PC) micellar solutions in D_2O . The solid lines are the fitted curves from the parameters listed in Table I.

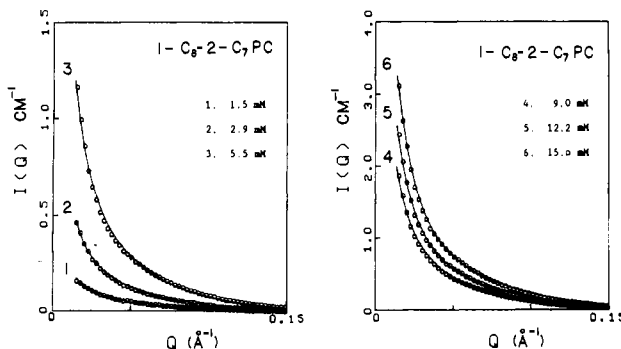


Figure 5. SANS data from 1-octanoyl-2-heptanoyl-PC (1- C_8 -2- C_7 -PC) micellar solutions in D_2O . The solid lines are the fitted curves from the parameters listed in Table I.

tanoyl-2-heptanoyl-PC. For each lecithin the key parameters ($(\Delta - N_0\delta)/kT$, δ/kT , N_0 , R_c , N/L) obtained from the fits of the model are listed in Table I.

For 1-heptanoyl-2-octanoyl-PC and 1-octanoyl-2-heptanoyl-PC systems the scattering intensity goes up to 40 or 50 cm^{-1} in the small- Q region for higher concentration samples. However, the experimental data used in the fitting covers a Q region only from 0.013 \AA^{-1} and up. To be sure that the parameters extracted from

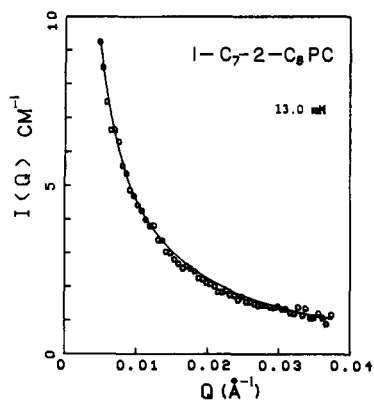


Figure 6. Open circles are the SANS experimental data covering a smaller Q region $0.005\text{--}0.04\text{ \AA}^{-1}$ from a D_2O solution containing 13.0 mM 1-heptanoyl-2-octanoyl-PC lecithin. The solid curve is the calculated behavior using the parameters, listed in Table I, determined from fitting the data shown in Figure 4, which covers the Q range $0.013\text{--}0.22\text{ \AA}^{-1}$.

the fitting are reliable without fitting any data below $Q = 0.013\text{ \AA}^{-1}$, neutron scattering data in the Q range $0.005\text{--}0.04\text{ \AA}^{-1}$ from a 13.0 mM 1-heptanoyl-2-octanoyl-PC solution taken at the HFIR, Oak Ridge National Laboratory, are compared with the predicted intensity computed by using the extracted parameters. Excellent agreement, as shown in Figure 6, is found between the predicted intensity and measured intensity even in this smaller Q region.

Figure 7 shows the plot of weight-averaged aggregation number vs. concentration for these asymmetric lecithin micellar systems. For 1-hexanoyl-2-heptanoyl-PC micelles, the mean aggregation number is found to increase from 34 to 44 as the concentration is increased from 7 to 35.1 mM (Figure 7A). The growth is noticeable for this asymmetric species compared to dihexanoyl-PC micelles, but it is still small compared to the growth of diheptanoyl-PC micelles,⁸ which grow from a mean aggregation number of 48 to 193 as the concentration was increased from 2.2 to 35.0 mM .⁸ The growth of 1-hexanoyl-2-octanoyl-PC and 1-octanoyl-2-hexanoyl-PC micelles with increasing concentration (Figure 7B) is comparable to the diheptanoyl-PC micellar system. The growth rate of 1-octanoyl-2-hexanoyl-PC micelles is lower than that of 1-hexanoyl-2-octanoyl-PC, and the mean aggregation number at the same concentration is smaller for 1-octanoyl-2-hexanoyl-PC. The same tendency is found for 1-octanoyl-2-heptanoyl-PC micelles compared with 1-heptanoyl-2-octanoyl-PC micelles, as shown in Figure 7C. The sizes of the micelles formed by 1-heptanoyl-2-octanoyl-PC or 1-octanoyl-2-heptanoyl-PC are much larger than those formed by the lecithins with 14 carbons in their fatty acyl chains. The mean aggregation number is on

the order of thousands in a concentration range $2\text{--}15\text{ mM}$. The size is more than 10 times larger than the size of micelles formed by 1-hexanoyl-2-octanoyl-PC or 1-octanoyl-2-hexanoyl-PC in the same concentration range.

The comparative growth rates are best illustrated by plotting the mean aggregation number vs. the square root of $X - X_1$ as shown in Figure 8. These curves are close to straight lines with slopes close to $2 \exp[(\Delta - N_0\delta)/2kT]$ according to the thermodynamic theory for micellar growth. Thus a slight difference in the value of $(\Delta - N_0\delta)/kT$ would cause a great difference in the mean aggregation number.

Another way to examine the dependence of growth rate for different species of lecithins is to look at the values of $(\Delta - N_0\delta)/kT$ for each species (Figure 9). Values for $(\Delta - N_0\delta)/kT$ can be classified according to the total carbon atoms in the fatty acyl chains of each lecithin species. The 14-carbon species diheptanoyl-PC, 1-hexanoyl-2-octanoyl-PC, and 1-octanoyl-2-heptanoyl-PC are in one group with similar values of $(\Delta - N_0\delta)/kT$ (TDF), ca. 16, while the 15-carbon species 1-heptanoyl-2-octanoyl-PC and 1-octanoyl-2-heptanoyl-PC are in another group with TDF values around 23. 1-Hexanoyl-2-heptanoyl-PC has 13 carbons in its chains and has a TDF = 12.086. The values of TDF roughly have a linear relationship with the number of fatty acyl carbon atoms as shown in Figure 9 by the broken line. This behavior predicts the TDF to be equal to 7 for dihexanoyl-PC micelles and about 28 for dioctanoyl-PC micelles. The weight-averaged mean aggregation number of dihexanoyl-PC micelles determined by SANS remained at 19 ± 1 from 27 to 360 mM .⁷ The growth rate is at most from $\bar{N} = 18$ to $\bar{N} = 20$ in this concentration range. The value of TDF can then be estimated to be about 7 or less. As for dioctanoyl-PC micelles there is no reliable data, since phase separation occurs at room temperature when salts are not added to suppress it.^{3,10} With a value of TDF around 28 for dioctanoyl-PC species, the micelles are predicted to grow into extremely large rod-like aggregates even at a few millimolar concentration. The interaction between these very large rod-like micelles cannot be neglected even at very low concentrations. In general one has the idea that TDF will increase about 5 when the tails have one more methylene group added.

The increase in TDF is in conjunction with the increase of the hydrocarbon core size when the volume of the tails is increased by adding more methylene groups to them. The size (minor radii) of the hydrocarbon core can be and must be increased to accommodate the larger tails. The result is that the surface area of the hydrocarbon core is thus increased, and the difference between the total surface area of the two end caps and the surface area of the same number of monomers in the straight section is thus increased. TDF can be considered as proportional to this

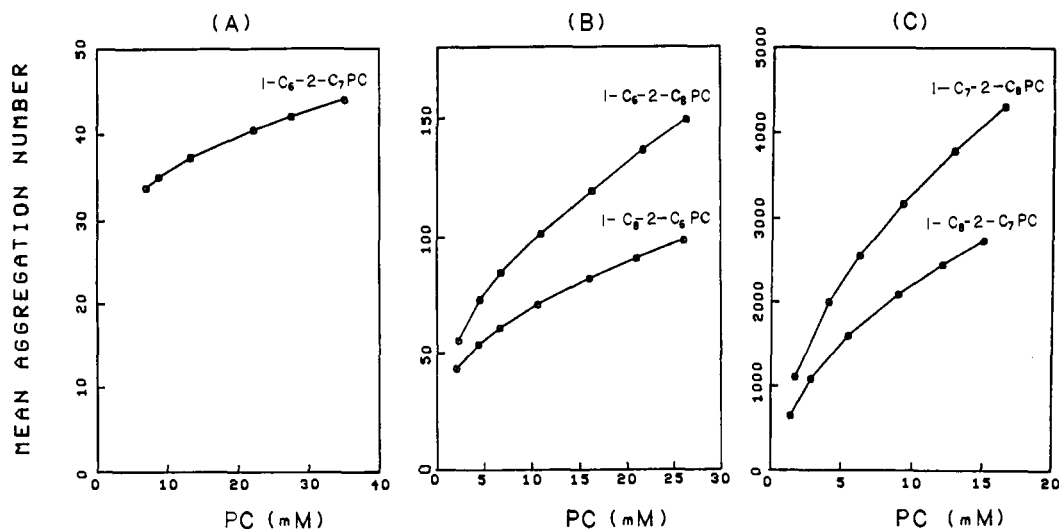


Figure 7. The weight-averaged aggregation number (\bar{N}) determined by fitting the experimental data is plotted vs. the lecithin concentration for (A) 1-hexanoyl-2-heptanoyl-PC, (B) 1-hexanoyl-2-octanoyl-PC and 1-octanoyl-2-hexanoyl-PC, and (C) 1-heptanoyl-2-octanoyl-PC and 1-octanoyl-2-heptanoyl-PC.

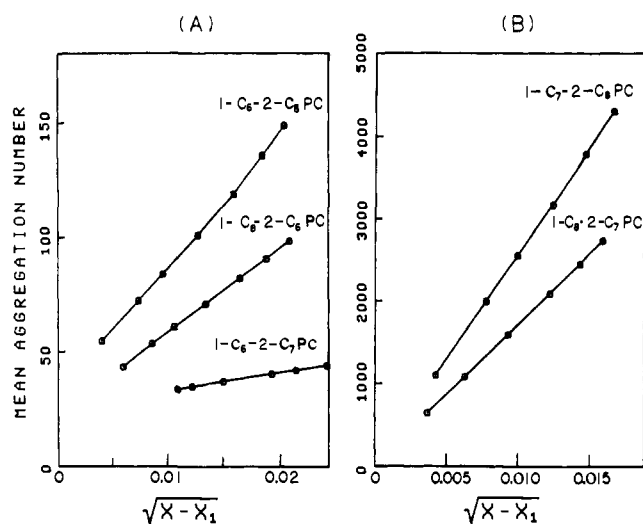


Figure 8. The weight-averaged aggregation number, \bar{N} , is plotted vs. $(X - X_1)^{1/2}$ for (A) 1-hexanoyl-2-heptanoyl-PC, 1-hexanoyl-2-octanoyl-PC, and 1-octanoyl-2-hexanoyl-PC and (B) 1-heptanoyl-2-octanoyl-PC and 1-octanoyl-2-heptanoyl-PC. The slopes of the lines are approximately equal to $2[\exp(\Delta - N_0\delta)/kT]^{1/2}$.

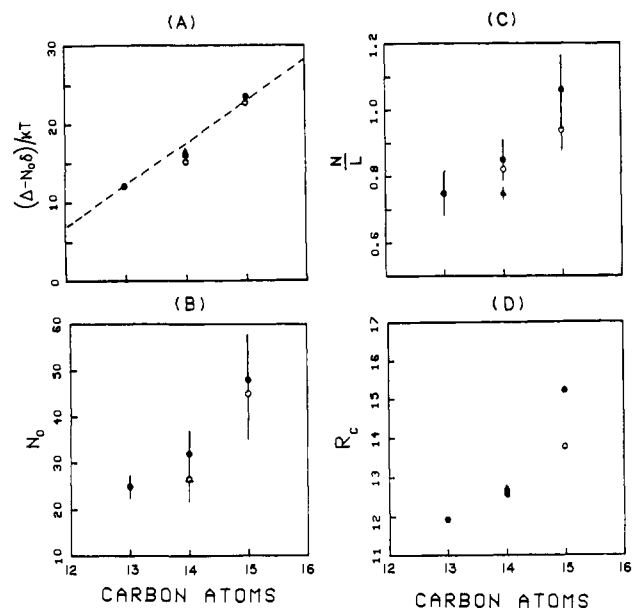


Figure 9. The following parameters for spherocylindrical short-chain lecithin micelles, determined from fitting the SANS data, are plotted vs. the total number of carbon atoms in the two fatty acyl chains: (A) $(\Delta - N_0\delta)/kT$; (B) N_0 , the number of monomers in the two end caps (minimum size micelle); (C) R_c (\AA), the transverse radius of gyration; (D) N/L (\AA^{-1}), the aggregation number per unit micelle length. Asymmetric lecithins with the S_{N1} chain shorter than its S_{N2} chain are represented by filled circles while the lecithins with the S_{N1} chain longer than its S_{N2} chain are represented by open circles. The diheptanoyl-PC is represented by filled triangles.

surface area difference with a constant hydrophobic interfacial free energy per unit area.

S_{N1}/S_{N2} Chain Nonequivalence. The actual dependence of TDF on the species of lecithins is far more complicated than this general rule. TDF values have been determined in great accuracy from fitting the SANS data since it is a very sensitive parameter in determining the micelle size. In Figure 9 TDF values for asymmetric lecithins with the S_{N1} chain shorter than its S_{N2} chain are represented by filled circles while the lecithins with the S_{N1} chain longer than its S_{N2} chain are represented by open circles. It can be seen that TDF values are higher for lecithins with shorter S_{N1} chains. The same ordering is also found in other parameters such as N_0 , R_c , and N/L as shown in Figure 9 (although R_c 's of 14-carbon lecithins are essentially identical). This indicates that

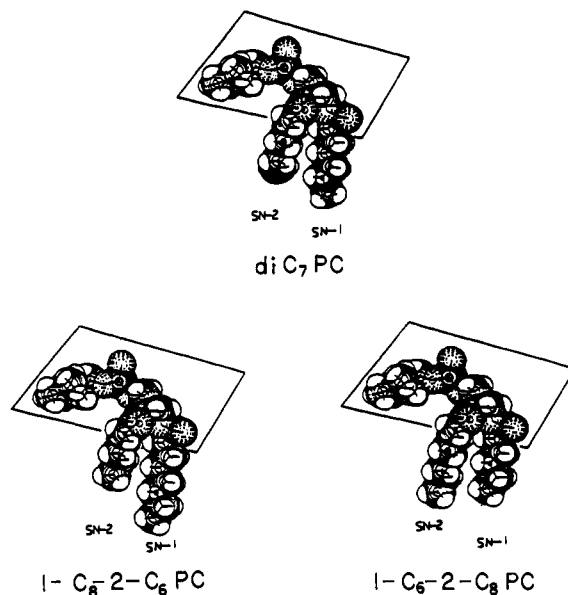


Figure 10. Space-filling representations of the shape of the diheptanoyl-PC, 1-octanoyl-2-hexanoyl-PC, and 1-hexanoyl-2-octanoyl-PC lecithins. The shape of the tails of 1-octanoyl-2-hexanoyl-PC lecithin is wedge-like and can be packed most easily in small micelles. The 1-hexanoyl-2-octanoyl-PC lecithin tails are more cylindrical in shape and hence are less easy to pack in small micelles compared with the 1-octanoyl-2-hexanoyl-PC lecithin. The boxes indicate the zwitterionic head group, glycerol backbone, and carbonyl moieties of the molecules.

1-octanoyl-2-hexanoyl-PC can be packed more easily to form micelles than 1-hexanoyl-2-octanoyl-PC, the same for 1-octanoyl-2-heptanoyl-PC compared with 1-heptanoyl-2-octanoyl-PC. This can be understood by considering the shape of these asymmetric lecithins. Figure 10 shows the space-filling representations of diheptanoyl-PC, 1-octanoyl-2-hexanoyl-PC, and 1-hexanoyl-2-octanoyl-PC in conformations consistent with the crystal structure of dimyristoylphosphatidylcholine in bilayers.¹¹ The S_{N1} acyl chain and the S_{N2} acyl chain (after an initial kink) are in all-trans conformations in these models. The longer S_{N1} chain and the most pronounced mismatch with the S_{N2} acyl chain gives the hydrophobic region of 1-octanoyl-2-hexanoyl-PC a more wedge-like shape than either the symmetric diheptanoyl-PC or the asymmetric 1-hexanoyl-2-octanoyl-PC species. Since all three molecules have the same polar headgroup, the one with the most wedge-shaped hydrocarbon region, i.e., 1-octanoyl-2-hexanoyl-PC, would be expected to pack into the smallest micelles. On the basis of the lecithin crystal structure, 1-hexanoyl-2-octanoyl-PC, where the two fatty acyl chains have nearly equivalent lengths, might be expected to form the largest micelles. Experimentally, diheptanoyl-PC forms the largest micelles. This indicates that an all-trans acyl chain is unlikely. The S_{N2} chain of a symmetric lecithin must be slightly shorter than the S_{N1} chain because the initial part of the S_{N2} chain is parallel, not perpendicular, to the interface. In the crystal structure of the longer lecithin this amounts to a 1.5- \AA carbon-carbon bond length between the ends of the two chains. Preferential introduction of gauche conformations into the S_{N1} chain would decrease the difference in the two acyl chains. For diheptanoyl-PC the difference should be less than one carbon-carbon bond length (ca. 1.3 \AA), because moving one methylene group from the S_{N1} chain of diheptanoyl-PC to the S_{N2} chain can form the better packed 1-hexanoyl-2-octanoyl-PC. This difference in chain packing is also sensed by ^1H chemical shifts of the S_{N1} and S_{N2} methyl groups. For the 14-carbon lecithins, the chemical shift difference at 500 MHz is largest for 1-octanoyl-2-hexanoyl-PC (Table II), still noticeable for 1-hexanoyl-2-octanoyl-PC, and much smaller for the symmetric species, diheptanoyl-PC. A similar ordering is observed for the S_{N1}/S_{N2} chemical shift difference for the 1-octanoyl-2-heptanoyl-PC and 1-heptanoyl-2-octanoyl-PC pair. This magnetic nonequivalence of the methyl groups reflects environmental dif-

Table II. ^1H NMR (500-MHz) Chemical Shift Differences of $\text{S}_{\text{N}1}$ and $\text{S}_{\text{N}2}$ α -Methylene and Methyl Groups in Short-Chain Lecithin Micelles

lecithin ^a	$\Delta_{\alpha\text{-CH}_2}$, Hz	Δ_{CH_3} , Hz
1-C ₆ -2-C-PC	33.5 ± 2.3	3.3 ± 0.8
(C ₇) ₂ -PC	35.0 ± 1.5	4.0 ± 1.0
1-C ₈ -2-C ₆ -PC	36.4 ± 2	18.6 ± 2.0
1-C ₆ -2-C ₈ -PC	31.9 ± 1.1	9.2 ± 1.9
1-C ₈ -2-C ₇ -PC	36.9 ± 1.8	5.9 ± 1.0
1-C ₇ -2-C ₈ -PC	33.2 ± 2.0	≤2

^a Abbreviations as in Table I.**Table III.** Comparison of Critical Micellar Concentrations (CMC) of Asymmetric Linear Short-Chain Lecithin Micelles Determined by SANS and ^1H NMR

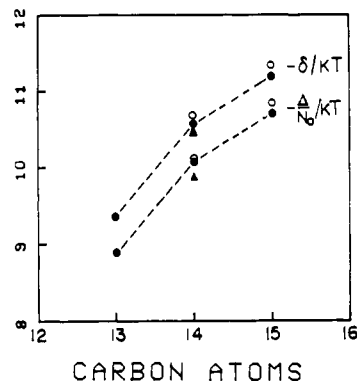
lecithin ^a	CMC, mM	
	SANS	NMR
1-C ₆ -2-C ₇ -PC	4.4 ± 0.1	4.9 ± 0.8
1-C ₆ -2-C ₈ -PC	1.4 ± 0.1	1.9 ± 0.5
1-C ₈ -2-C ₆ -PC	1.25 ± 0.1	1.5 ± 0.2
1-C ₇ -2-C ₈ -PC	0.76 ± 0.1	0.53 ± 0.03
1-C ₈ -2-C ₇ -PC	0.66 ± 0.1	0.58 ± 0.05

^a Abbreviations as noted in Table I.

ferences of chain termini and suggests that in micelles the average chain conformations are such that the terminal methyls have the same environment for the symmetric species.

CMC Values for Asymmetric Lecithins. $-\delta$ is the lowering of free energy per monomer when free monomers form the straight section of the spherocylindrical micelle, and $-\Delta/N_0$ is the lowering of free energy per monomer when free monomers form the end caps of the micelle. $-\delta/kT$ is related to the free monomer concentration in the solution through $X_1 = \beta e^{\delta/kT}$. For micellar systems with fast growth rate β is always very close to unity (as for 1-heptanoyl-2-octanoyl-PC and 1-octanoyl-2-heptanoyl-PC). In these cases the CMC (in mole fraction) is very close to $e^{\delta/kT}$. A sharp CMC exists for high TDF cases,²⁰ for example, 1-heptanoyl-2-octanoyl-PC or 1-octanoyl-2-heptanoyl-PC systems, and the CMC can be defined by $(X/X_1)_{X=X_{\text{cmc}}} = 1.001$ or simply by taking $X_{\text{cmc}} = e^{\delta/kT}$. For other cases with smaller TDF values and thus less sharp CMC, the CMC can be defined by $X/X_1 = 1.05$ at $X = X_{\text{cmc}}$ and can be computed from the fitted parameters N_0 , δ/kT , and $(\Delta - N_0\delta)/kT$. The CMC values extrapolated from SANS data for the asymmetric lecithins are listed in Table III and compared with the CMC values determined by ^1H NMR. The agreement between the results are within the measurement uncertainties. The CMC values determined by NMR are more accurate for PCs with 14 or more carbons in the fatty acyl chains since the chemical shift difference between monomer and micelle is more pronounced. The CMC of 1-octanoyl-2-hexanoyl-PC is smaller than that of 1-hexanoyl-2-octanoyl-PC; this is also true for 1-octanoyl-2-heptanoyl-PC and 1-heptanoyl-2-octanoyl-PC pairs. A smaller CMC and also a larger $|\delta|$ both indicate that lecithins with longer $\text{S}_{\text{N}1}$ chains can be more easily packed into micelles than species with the chains switched. It is also consistent with the initial part of the $\text{S}_{\text{N}2}$ chain oriented at the interface, hence not contributing as much to the hydrophobicity of the molecule. This type of behavior was seen previously with methyl-branched short-chain lecithins.¹⁰ Diheptanoyl-PC is more like 1-hexanoyl-2-octanoyl-PC in its CMC and $|\delta|$.

Free Energy/Monomer for End Caps vs. Cylindrical Section. Figure 11 shows the plots of $-\delta/kT$ and $(-\Delta/N_0)/kT$ vs. the number of atoms in the two fatty acyl chains. Both of these two parameters vary in a similar way with different species of lecithins. The difference between $-\delta/kT$ and $(-\Delta/N_0)/kT$ is roughly the same, about 0.5 kT per monomer, for all species. Adding one methylene group to the tails will increase $-\delta$ or $-\Delta/N_0$ about 1 kT , but the exact dependence is more involved. The increment of $-\delta/kT$ or $(\Delta/N_0)/kT$ from 14-carbon lecithins to 15-carbon

**Figure 11.** Values of $-\delta/kT$ and $(-\Delta/N_0)/kT$ determined in this study are plotted vs. the total carbon atoms in the tails for each lecithin species.**Table IV.** Computed Structural Parameters of the Spherocylindrical Short-Chain Lecithin Micelles

lecithin ^a	a_r , Å	R_{core} , Å	$R_{\text{c,head}}$, Å	$R_{\text{c,head}} - R_{\text{core}}$, Å	V_{tail} , Å ³
1-C ₆ -2-C ₇ -PC	25.0	9.15	17.1	8.0 ± 1	350.7
(C ₇) ₂ -PC	27.0	9.5	18.7	9.2 ± 0.5	377.6
1-C ₆ -2-C ₈ -PC	28.3	10.1	18.2	8.1 ± 0.5	377.6
1-C ₈ -2-C ₆ -PC	24.8	9.9	18.4	8.5 ± 0.5	377.6
1-C ₇ -2-C ₈ -PC	34.0	11.7	22.7	11.0 ± 1.5	404.5
1-C ₈ -2-C ₇ -PC	34.0	11.3	20.2	8.9 ± 1.0	404.5

^a Abbreviations as in Table I.

lecithins is smaller than the increment from 13-carbon lecithins to 14-carbon lecithins. It may imply that the longer 15-carbon lecithins (1-heptanoyl-2-octanoyl-PC or 1-octanoyl-2-heptanoyl-PC) need more (fractional) gauche conformations, which cost extra energy, in packing the tails in the micelle core. A general rule shows that the surface area of the hydrocarbon core sustained by each monomer is roughly independent of the tail length.²¹ Thus the smaller increment in $-\delta$ or $-\Delta/N_0$ could be mainly due to the entropic factor and the difference in conformation energy.

Structure of the Hydrocarbon Core. The aggregation number per unit micelle length N/L can be used to compute the radius of the hydrocarbon core R_{core} of the straight section. Assuming a close packed cylindrical core, one has the relation

$$\pi R_{\text{core}}^2 = V_{\text{tail}} \frac{N}{L} \quad (8)$$

Using the averaged values of N/L for each species of lecithins and the Tanford's empirical formula for V_{tail} ,²² one can compute R_{core} from eq 8. R_{core} is found to be equal to 9.2, 9.5, 10.1, 9.9, 11.7, and 11.3 Å for 1-hexanoyl-2-heptanoyl-PC, diheptanoyl-PC, 1-hexanoyl-2-octanoyl-PC, 1-octanoyl-2-hexanoyl-PC, 1-heptanoyl-2-octanoyl-PC, and 1-octanoyl-2-heptanoyl-PC micelles, respectively. 1-Octanoyl-2-heptanoyl-PC and 1-octanoyl-2-hexanoyl-PC can be packed more easily and have smaller R_{core} 's compared with their asymmetric counterparts. The values of R_{core} are larger for lecithins with 15 carbons in their fatty acyl chains compared with the lecithins with 14 carbons in their fatty acyl chains. Since both the lengths and the volumes of the fatty acyl chains are larger, the 15-carbon lecithins can have and need to have a larger R_{core} to accommodate the fatty acyl chains. In comparison with the diheptanoyl-PC, the same 14-carbon asymmetric lecithins, 1-hexanoyl-2-octanoyl-PC and 1-octanoyl-2-hexanoyl-PC, have larger values of R_{core} because the lengths of their fatty acyl chains are larger. Some of the values of R_{core} of these lecithins exceed the length of their fatty acyl chains, and the cross sectional area of their hydrocarbon core must deviate slightly from a circular form (presumably forming ellipses).

(21) Tausk, R.; Overbeek, J. Th. G. *Colloid Interface Sci.*, [Proc. Int. Conf.], 50th 1976, 2, 379.(22) Tanford, C. *The Hydrophobic Effect*, 2nd ed.; Wiley: New York, 1980.(20) Mukerjee, P. *J. Phys. Chem.* 1972, 76, 565.

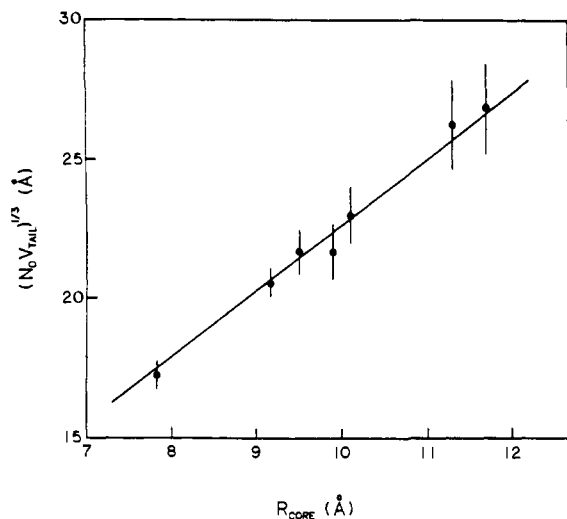


Figure 12. The relation between N_0 and the averaged hydrocarbon core radius R_{core} of the spherocylindrical micelles can be shown by plotting $(N_0 V_{\text{tail}})^{1/3}$ vs. R_{core} . The linear relationship is shown by the straight line, which indicates that there is a similarity in the shape of the hydrocarbon portion of the end caps of all the lecithin micelle species studied.

The shape of the two end caps of the spherocylindrical core can be determined by using the values of V_{tail} and N_0 . The hydrocarbon core volume of the two end caps is equal to $N_0 V_{\text{tail}}$. A natural choice of the shape of the minimum size micelle, which is assumed to have the same shape as the end caps, is an ellipsoid with the minor radius equal to R_{core} . The major axis a is then determined from eq 9. The computed values of a and R_{core} are

$$\frac{4}{3}\pi a(R_{\text{core}})^2 = N_0 V_{\text{tail}} \quad (9)$$

listed in Table IV. The value of the major axis a varies from 25 to 34 Å. One interesting finding is that $(N_0 V_{\text{tail}})^{1/3}$ varies linearly with R_{core} as shown in Figure 12. All the points in Figure 12 fit well to the following relation

$$(N_0 V_{\text{tail}})^{1/3} = 2.22 R_{\text{core}} \quad (10)$$

Comparing eq 10 with eq 9, one finds that the ratio a/R_{core} is a constant, 2.61, for all the lecithin micelles. This means that a geometrical similarity exists among all of the end caps of different lecithin micelles or among all of the minimum size micelles formed by different lecithins.

Orientation of Lecithin Head Groups. From the values of the transverse radius of gyration R_c and the values of R_{core} , one can calculate the transverse radius of gyration of the head group, denoted by $R_{c,\text{head}}$, by using the methods described earlier.⁷ The computed results of $R_{c,\text{head}}$ are listed in Table IV together with the values of $R_{c,\text{head}} - R_{\text{core}}$, which is an indication of the distance of the weighted head group scattering center from the surface of the hydrocarbon core. This distance is found to be about 9 ± 1 Å for all lecithin micelles. Since the choline moiety represents the head group scattering center, this implies that in short-chain lecithin micelles the phosphocholine head group must be parallel to the interface.

Hydrocarbon Core Surface Area. Finally, the hydrocarbon core surface area sustained by each monomer can be computed from the known micellar structure by using the values of a and R_{core} . This core surface area per monomer is listed in Table V for lecithins in the straight section and in the end caps too. The core surface area in the straight section, 70–80 Å²/monomer, is only slightly larger than the area per molecule in a monolayer, about 60 Å².¹ The core surface area in the end caps is larger than that in the straight section by about 16–19 Å² when one assumes that end caps are half ellipsoids. The difference between Δ/N_0 and δ is largely due to the difference in the hydrophobic interfacial energy and thus is proportional to the difference in the surface area in the end caps and in the straight section. One can then estimate the interfacial free energy by dividing $\Delta/N_0 - \delta$ by the reduction in surface area and hence obtain roughly a constant

Table V. Computed Hydrocarbon Core Surface Area per Monomer and Estimated-Hydrophobic Interfacial Free Energy per Unit Area

lecithin ^a	A_{EC}^b , Å ²	A_{SS}^c , Å ²	$A_{\text{EC}} - A_{\text{SS}}$, Å ²	$(\Delta - N_0\delta)/(A_{\text{EC}} - A_{\text{SS}})$, $kT/\text{Å}^2$
1-C ₆ -2-C-PC	94.5	76.2	18.3	0.0264 ± 5%
(C ₇) ₂ -PC	98.2	79.5	18.7	0.0326 ± 5%
1-C ₆ -2-C ₈ -PC	92.4	74.5	17.7	0.0284 ± 5%
1-C ₈ -2-C ₆ -PC	95.4	76.5	18.9	0.0297 ± 5%
1-C ₇ -2-C ₈ -PC	85.3	70.3	16.0	0.0306 ± 10%
1-C ₈ -2-C ₇ -PC	87.9	71.5	16.4	0.0307 ± 10%

^a Abbreviations as in Table I. ^b A_{EC} : hydrocarbon core surface area per monomer in the end caps of spherocylindrical micelles. ^c A_{SS} : hydrocarbon core surface area per monomer in the straight section of spherocylindrical micelles.

number $0.03kT/\text{Å}^2$ for all lecithins, as listed in Table V. The detailed difference between species may be due to slight variations in surface smoothness and in conformation or entropic energies. This number $0.03kT/\text{Å}^2$ is within the range of the generally estimated hydrophobic interfacial energy $0.03\text{--}0.04kT/\text{Å}^2$.^{19,23}

Summary and Discussion

The step and ladder model¹⁹ for the change in chemical potential in micellization and in micellar growth has been successfully applied to the analyses of SANS data from short-chain lecithin micellar solutions.⁸ The formation and growth of micelles can be characterized completely by three parameters, $(\Delta - N_0\delta)/kT$, δ/kT , and N_0 . This theory predicts that the growth rate in terms of $\bar{N}/(X - X_1)^{1/2}$ is roughly proportional to $2e^{(\Delta - N_0\delta)/2kT}$. All the short-chain lecithin micellar systems studied are found to follow this rule. It is also found that the radial structure of the micelle is the same for all the micelles of the same species. The radial structure can be characterized by two parameters, R_c and N/L . By fitting the SANS data to the model, one can extract the five parameters for each lecithin micellar system.

In general the lecithin micelles grow with increasing concentration. The size distribution becomes very wide and thus becomes polydispersed when micelles start to grow beyond the minimum size. In the high concentration limit the ratio of the weight-averaged aggregation number to the number-averaged aggregation number approaches 2.⁸ The fatty acyl chains of the lecithins form a close packed hydrocarbon core of a spherocylindrical shape. The radius of the core can be determined from SANS studies, and the results show that their values depend on the size and structure of the fatty acyl chains. All the lecithin micelles studied have a geometrical similarity among their end caps. The number of monomers in the two end caps, N_0 , is found to have a universal relation with the averaged core radius R_{core} , as given by eq 10, for all the lecithin micelles studied here. The weighted scattering center of the head groups is found to be at a distance of about 9 ± 1 Å from the hydrocarbon core surface, implying that the phosphocholine group is not extended from the surface but is more likely parallel to the hydrocarbon surface.

The values of $(\Delta - N_0\delta)/kT$ are found to vary: 7 for dihexanoyl-PC, 12 for 1-hexanoyl-2-heptanoyl-PC, 16 for the 14-carbon lecithins (diheptanoyl-PC, 1-hexanoyl-2-octanoyl-PC, and 1-octanoyl-2-hexanoyl-PC), and 23 for the 15-carbon lecithin micelles (1-heptanoyl-2-octanoyl-PC and 1-octanoyl-2-heptanoyl-PC). The origin of $\Delta - N_0\delta$ is thought to be largely due to the difference in the total hydrophobic interfacial free energy for the monomers in the two end caps and for the same number of monomers in the straight section. This interfacial hydrophobic free energy is found to be about $0.03kT/\text{Å}^2$, assuming the hydrocarbon cores of the end caps are half ellipsoids. The exact values of $(\Delta - N_0\delta)/kT$ vary with lecithin species. If the lecithin tails can be more easily packed into the hydrocarbon core of the micelle, micelle growth is much less pronounced with increasing lecithin concentration.

For molecules with two short fatty acyl chains, the packing of the tails into a close packed core is very different from the situation

for molecules with a single long chain. Both chains are found to be important in the packing. Differences in micelle characteristics for lecithins with the same total carbon atoms in the fatty acyl chains reflect the nonequivalence of the two fatty acyl chains. While the S_N1 and S_N2 chains are not equivalent in packing in the disordered micelle hydrocarbon core,⁷ this difference is found to be less than that in the bilayer structure. Finally, the form factor of these rod-like short-chain lecithin micelles can be approximately taken to be that of a rigid rod even when they grow up to a length of a few thousand angstroms, having a length to diameter ratio larger than 100. This point is inferred from the constant R_c and N/L values found for each lecithin species at all the concentrations studied.

The detailed structures of short-chain lecithin micelles are useful for understanding hydrolysis rates of water-soluble phospholipases. These enzymes show higher specific activities toward micellar lecithins than toward lecithins packed in a bilayer. It has been suggested that this may be due to the larger area per head group, i.e., greater accessibility, of lecithins in micelles ($\approx 100 \text{ \AA}^2$ for dihexanoyl-PC) compared to those in bilayers ($\approx 65 \text{ \AA}^2$). For

short-chain lecithins with 14 or more carbons in the fatty acyl chains, the micelles are long spherocylinders. While head group areas are $90\text{--}95 \text{ \AA}^2$ in the end caps, the majority of the lecithin molecules are in the long rod sections with considerably smaller head group areas ($70\text{--}75 \text{ \AA}^2$). Since phospholipase C from *Bacillus cereus* has essentially the same activity toward all these short-chain lecithins, substrate head group area alone is probably not the major cause of the activity difference between micelles and bilayer packed lecithins.

Acknowledgment. We are grateful to Dr. Benno Schoenborn of the Biology Department of Brookhaven National Laboratory for granting sufficient beam time for the experiment and to Dr. D. K. Schneider for assistance in using the Biology low-angle neutron spectrometer. We would also like to thank Drs. W. C. Koehler, G. D. Wignall, and J. Hayter for help in using the 30-M SANS spectrometer at NCSASR, ORNL. This research is supported by a NSF grant administrated through the Center for Materials Science and Engineering (S.-H.C.) and NIH Grant GM26762 (M.F.R.).

Nuclear Relaxation in the Magnetic Coupled System $\text{Cu}_2\text{Co}_2\text{SOD}$. Histidine-44 Is Detached upon Anion Binding

L. Banci, I. Bertini,* C. Luchinat, and A. Scozzafava

Contribution from the Department of Chemistry, University of Florence, Florence, Italy.
Received June 19, 1986

Abstract: The ^1H NMR spectra of bovine erythrocyte superoxide dismutase in which zinc is substituted by cobalt ($\text{Cu}_2\text{Co}_2\text{SOD}$) have been recorded at 60, 90, 200, and 400 MHz and compared with those already reported at 300 MHz. The experimental T_1 and T_2 values have been related to the experimental (from X-ray) metal proton distances, thus obtaining a detailed assignment of the signals and the electronic relaxation times (τ_s) of the two metal ions in the coupled system. This has required some critical considerations on the available theory since no such approach had been attempted before on a magnetically coupled system. Comparison of $\text{Cu}_2\text{Co}_2\text{SOD}$ with $\text{Cu}_2\text{Zn}_2\text{SOD}$, on the one hand, and with $\text{E}_2\text{Co}_2\text{SOD}$ (E = empty), on the other, has shown that in the coupled system τ_s of copper is decreased by two orders of magnitude and that of cobalt by a factor of 3. The ^1H NMR spectra at 300 MHz for the N_3^- derivative have been reanalyzed and the T_1 values have been measured. It is shown that His-44 is the one which undergoes detachment upon anions binding, since the isotropic shifts of its protons vanish. However, some paramagnetic effect is measured on T_1 which allowed us to envisage the new position of His-44 within the protein.

Bovine erythrocyte superoxide dismutase is a dimeric protein of MW 32 000, with each subunit containing a catalytically essential copper ion bridged by an histidinato residue to a solvent inaccessible zinc ion ($\text{Cu}_2\text{Zn}_2\text{SOD}$). Figure 1 schematically shows the spatial arrangement of the resulting dimetallic cluster as it appears from the 2- \AA resolution X-ray structure.¹ It has been shown that zinc(II) can be replaced by cobalt(II)²⁻⁴ with virtually no alteration of the coordination geometry of the copper ion⁵ and of the catalytic properties of the enzyme⁶ ($\text{Cu}_2\text{Co}_2\text{SOD}$). This "innocent" substitution has, however, dramatic effects on the spectroscopic properties of the resulting derivative: magnetic

exchange coupling interactions between the high-spin cobalt(II) and the copper(II) centers take place, with an isotropic exchange coupling constant of 16.5 cm^{-1} (i.e., a separation of 33 cm^{-1} between the $S = 2$ and $S = 1$ multiplets, the latter being lower).⁷ This results in a dramatic shortening of the electronic relaxation times of copper(II) and therefore in the disappearance of its EPR spectrum. On the other hand, this allowed us to observe the ^1H NMR signals of the ring protons of the histidines coordinated to both the cobalt(II) and the copper(II) chromophores.⁵ Therefore, exchange coupling with cobalt(II) turns the copper(II) ion into a potentially precious NMR probe for the investigation of the system. For instance, it has been observed that upon addition of azide or cyanate, which are known to bind copper on the native protein,⁸⁻¹⁰ some of the isotropically shifted signals move toward

(1) Tainer, J. A.; Getzoff, E. D.; Beem, K. M.; Richardson, J. S.; Richardson, D. C. *J. Mol. Biol.* **1982**, *160*, 181-217.

(2) Fee, J. A. *J. Biol. Chem.* **1973**, *248*, 4229-4234.

(3) Calabrese, L.; Rotilio, G.; Mondovì, B. *Biochim. Biophys. Acta* **1972**, *263*, 827-829.

(4) Calabrese, L.; Cocco, D.; Morpurgo, L.; Mondovì, B.; Rotilio, G. *Eur. J. Biochem.* **1976**, *64*, 465-470.

(5) Bertini, I.; Lanini, G.; Luchinat, C.; Messori, L.; Monnanni, R.; Scozzafava, A. *J. Am. Chem. Soc.* **1985**, *107*, 4391-4396.

(6) Beem, K. M.; Rich, W. E.; Rajagopalan, K. V. *J. Biol. Chem.* **1974**, *249*, 7298-7305.

(7) Morgenstern-Badarau, I.; Cocco, D.; Desideri, A.; Rotilio, G.; Jordanov, J.; Dupre, N. *J. Am. Chem. Soc.* **1986**, *108*, 300-302.

(8) Rotilio, G.; Finazzi Agrò, A.; Calabrese, L.; Bossa, F.; Guerrieri, P.; Mondovì, B. *Biochemistry* **1971**, *10*, 616-621.

(9) Fee, J. A.; Gaber, B. P. *J. Biol. Chem.* **1972**, *247*, 60-65.

(10) Bertini, I.; Borghi, E.; Luchinat, C.; Scozzafava, A. *J. Am. Chem. Soc.* **1981**, *103*, 7779-7783.